



## A dual-chain assembly pathway generates the high structural diversity of cell-wall polysaccharides in *Lactococcus lactis*

Ilias Theodorou, Pascal Courtin, Simon Palussière, Saulius Kulakauskas, Elena Bidnenko, Christine Péchoux, François Fenaille, Christophe Penno, Jennifer Mahony, Douwe van Sinderen, et al.

### ► To cite this version:

Ilias Theodorou, Pascal Courtin, Simon Palussière, Saulius Kulakauskas, Elena Bidnenko, et al.. A dual-chain assembly pathway generates the high structural diversity of cell-wall polysaccharides in *Lactococcus lactis*. Journal of Biological Chemistry, 2019, 294 (46), pp.17612-17625. 10.1074/jbc.RA119.009957 . hal-03343068

**HAL Id: hal-03343068**

**<https://hal.inrae.fr/hal-03343068>**

Submitted on 14 Sep 2021

**HAL** is a multi-disciplinary open access archive for the deposit and dissemination of scientific research documents, whether they are published or not. The documents may come from teaching and research institutions in France or abroad, or from public or private research centers.




L'archive ouverte pluridisciplinaire **HAL**, est destinée au dépôt et à la diffusion de documents scientifiques de niveau recherche, publiés ou non, émanant des établissements d'enseignement et de recherche français ou étrangers, des laboratoires publics ou privés.



Distributed under a Creative Commons Attribution 4.0 International License

# A dual-chain assembly pathway generates the high structural diversity of cell-wall polysaccharides in *Lactococcus lactis*

Received for publication, June 26, 2019, and in revised form, September 30, 2019. Published, Papers in Press, October 3, 2019; DOI 10.1074/jbc.RA119.009957

Ilias Theodorou<sup>‡§</sup>, Pascal Courtin<sup>¶</sup>, Simon Palussière<sup>¶</sup>, Saulius Kulakauskas<sup>¶</sup>,  Elena Bidnenko<sup>¶</sup>, Christine Péchoux<sup>¶</sup>,  François Fenaille<sup>\*\*</sup>, Christophe Penno<sup>‡§</sup>, Jennifer Mahony<sup>‡§1</sup>, Douwe van Sinderen<sup>‡§2,3</sup>, and  Marie-Pierre Chapot-Chartier<sup>¶2,4</sup>

From the <sup>‡</sup>School of Microbiology and <sup>§</sup>APC Microbiome Ireland, University College Cork, Western Road, Cork, Ireland, <sup>¶</sup>Micalis Institute, INRA, AgroParisTech, Université Paris-Saclay, 78350 Jouy-en-Josas, France, <sup>¶</sup>INRA, UMR 1313 Génétique Animale et Biologie Intégrative (GABI), Plate-forme MIMA2, 78350 Jouy-en-Josas, France, and <sup>\*\*</sup>CEA, Institut Joliot, Service de Pharmacologie et d'Immunoanalyse, UMR 0496, Laboratoire d'Etude du Métabolisme des Médicaments, MetaboHUB-Paris, Université Paris-Saclay, 91191 Gif-sur-Yvette, France

Edited by Chris Whitfield

In *Lactococcus lactis*, cell-wall polysaccharides (CWPSs) act as receptors for many bacteriophages, and their structural diversity among strains explains, at least partially, the narrow host range of these viral predators. Previous studies have reported that lactococcal CWPS consists of two distinct components, a variable chain exposed at the bacterial surface, named polysaccharide pellicle (PSP), and a more conserved rhamnan chain anchored to, and embedded inside, peptidoglycan. These two chains appear to be covalently linked to form a large heteropolysaccharide. The molecular machinery for biosynthesis of both components is encoded by a large gene cluster, named *cwps*. In this study, using a CRISPR/Cas-based method, we performed a mutational analysis of the *cwps* genes. MALDI-TOF MS-based structural analysis of the mutant CWPS combined with sequence homology, transmission EM, and phage sensitivity analyses enabled us to infer a role for each protein encoded by the *cwps* cluster. We propose a comprehensive CWPS biosynthesis scheme in which the rhamnan and PSP chains are independently synthesized from two distinct lipid-sugar precursors and are joined at the extracellular side of the cytoplasmic membrane by a mechanism involving a membrane-embedded glycosyltransferase with a GT-C fold. The proposed scheme encompasses a system that allows extracytoplasmic modification of rhamnan by complex substituting oligo-/polysaccharides. It accounts for the extensive diversity of CWPS structures observed among lactococci and may also have relevance to the biosynthesis of complex rhamnase-containing CWPSs in other Gram-positive bacteria.

The surface of most bacteria is coated with polysaccharides (PSs)<sup>5</sup> of variable structures, including capsular polysaccharides (CPSs), cell-wall polysaccharides (CWPSs), and lipopolysaccharides, which are crucial for specific interactions of bacteria with their environment (1, 2). A high degree of structural diversity is typically observed in these polymers among bacterial species or even among strains of the same species, which is considered to be a consequence of environmental and biological pressures and which results from coevolution of bacteria with their eukaryotic host, their infecting phages, or other microorganisms in a complex microbiota (3). The chemical diversity of bacterial PSs is mirrored by the genetic diversity of the loci encoding the components of their biosynthetic apparatus.

Despite this high diversity, the general mechanisms of PS polymerization and export exhibit conserved features (4). The most common mechanisms are the Wzx/Wzy- and ATP-binding cassette (ABC) transporter pathways (5, 6). In both pathways, PS (subunit) synthesis is initiated on a lipid acceptor, most often undecaprenyl phosphate (Und-P), by addition of sugar-phosphate to form Und-PP-sugar, at the inner face of the cytoplasmic membrane. In the Wzx/Wzy-dependent pathway, following synthesis of individual PS repeat units linked to Und-P, they are exported by the flippase Wzx to the outside of the cytoplasmic membrane where they are then assembled into the mature PS by the polymerase Wzy. In the ABC transporter-dependent pathway, the entire PS chain is elongated on the lipid carrier before being translocated across the cytoplasmic membrane by an ABC transporter. In Gram-positive bacteria, CWPS or CPS chains can, subsequent to their translocation across the membrane, be covalently anchored onto peptidoglycan by proteins of the LytR-Cps2A-Psr (LCP) family (7).

The diversity of PS structures results from the wide variety of glycosyltransferases, which are involved in glycan chain elon-

The work of the M.-P. C.-C. team was supported by INRA. The authors declare that they have no conflict of interest with the contents of this article.

This article contains Figs. S1–S5 and Tables S1–S4.

<sup>1</sup> Recipient of Starting Investigator Research Grant (SIRG) 15/SIRG/3430 funded by Science Foundation Ireland (SFI).

<sup>2</sup> Both authors contributed equally to this work.

<sup>3</sup> Supported by Principal Investigator Award 450 13/IA/1953 through SFI. To whom correspondence may be addressed: School of Microbiology, University College Cork, Western Road, Cork, Ireland. Tel.: 353-21-4901365; E-mail: d.vansinderen@ucc.ie.

<sup>4</sup> To whom correspondence may be addressed: Micalis Institute, INRA, 78350 Jouy-en-Josas, France. Tel.: 33-1-34-65-22-68; E-mail: Marie-Pierre.Chapot-Chartier@inra.fr.

This is an Open Access article under the CC BY license.

17612 J. Biol. Chem. (2019) 294(46) 17612–17625

<sup>5</sup> The abbreviations used are: PS, polysaccharide; CWPS, cell-wall polysaccharide; PSP, polysaccharide pellicle; CPS, capsular polysaccharide; Und-P, undecaprenyl phosphate; Und-PP, undecaprenyl pyrophosphate; SEC, size-exclusion chromatography; TMH, transmembrane helix; TEM, transmission electron microscopy; LCP, LytR-Cps2A-Psr; Rha, rhamnose; TSS, transcription start site; TU, transcriptional unit; PGT, phosphoglycosyltransferase; AA, amino acids; GT, glycosyltransferase; ArnT, 4-amino-4-deoxy-L-arabinose (L-Ara4N) transferase; HF, hydrofluoric acid.

gation and show a high degree of specificity for both their donor and acceptor substrates. Moreover, structural diversity of glycoconjugates can also be increased by modifications added late in the biosynthesis pathway after translocation of the glycan chain across the cytoplasmic membrane. Three-component systems that carry out extracytoplasmic glycosylation of glycoconjugates have been described previously and are characterized by the involvement of polyprenyl monophosphoryl donors and GT-C fold glycosyltransferases (8). The typical three-component modification machinery involves: (i) a glycosyltransferase that transfers a particular sugar from an NDP-sugar donor to polyprenol-P carrier, generating a polyprenol-monophosphate-sugar at the inner face of the cytoplasmic membrane; (ii) a flippase to transport the polyprenol-P-sugar to the outer side of the membrane; and (iii) a polytopic membrane glycosyltransferase with a GT-C fold that completes the reaction by catalyzing the transfer of the sugar from polyprenol-P-sugar to the glycoconjugate substrate.

*Lactococcus lactis* is a bacterial species of tremendous economic importance, being extensively used in dairy fermentations (9). As a result, numerous bacteriophages infecting *L. lactis* have been isolated, constituting a major concern due to their detrimental effect on the quality of the final fermented food products. CWPSs with highly variable structures among *L. lactis* strains have been identified as receptors for phages of several families (10). Moreover, the observed differences in CWPS structure are, at least partially, responsible for the high degree of specificity of lactococcal phages and their observed narrow host range (11). To date, the CWPS chemical structures of five different *L. lactis* strains have been elucidated (Fig. S1). Based on genomic sequence analysis of the gene cluster encoding CWPS biosynthesis (*cwps* cluster), *L. lactis* strains have been classified into three distinct *cwps* genotypes, i.e. types A, B, and C (12). We have previously shown that, in C-type strains, CWPS consists of two components. The first of these, known as the polysaccharide pellicle (PSP), is made up of repeating oligosaccharide units linked by phosphodiester bonds and forms a thin outer layer exposed at the bacterial cell surface (13). PSP was found to exhibit structural diversity among C-type strains (11, 14). The second component is a rhamnan with a conserved structure and appears to be embedded within the peptidoglycan mesh (15). Our biochemical data furthermore suggest that rhamnan and PSP are covalently linked to form a single complex hetero-PS, which itself is covalently attached to peptidoglycan through its rhamnan part (15). More recently, CWPSs from both an A-type and a B-type strain were found to consist of a unique component made of a rhamnose-rich or rhamnan linear chain, respectively, substituted by short oligosaccharide chains (16, 17). Overall, *L. lactis* CWPSs can be classified in the family of rhamnose (Rha)-containing CWPSs that are also found in streptococci and enterococci (18). Of note, these Rha-containing CWPSs also appear to represent a major component of the cell wall, accounting for about half of its mass and having a crucial role in cell-wall architecture (15, 18–20).

The molecular machinery responsible for assembling CWPS, including both PSP and rhamnan for C-type strains, was mapped to the *cwps* gene cluster, which is ~25 kb in length (13)

and which exhibits a high level of sequence and gene content diversity among strains, particularly at its 3' end (11, 12, 15). Although it is established that the *L. lactis* NZ9000 *cwps* cluster is responsible for rhamnan and PSP biosyntheses, functional assignment is not available at present for each of the 22 proteins encoded by the gene cluster. Previously, we have proposed a model for rhamnan biosynthesis in *L. lactis* NZ9000 involving an ABC transporter–dependent pathway, assigning a function to nine proteins encoded in the 5' part of the *cwps* cluster (15). In contrast, little is known about PSP biosynthesis. In the current study, we have combined a mutational analysis of the *cwps* genes present in the C-type strain *L. lactis* NZ9000 with structural analysis of the mutant CWPS and bioinformatics analysis of the proteins encoded in the *cwps* cluster to propose an original model for PSP biosynthesis and linkage to rhamnan. Moreover, characterization of the constructed mutants by transmission EM and phage sensitivity assays support the proposed model.

## Results and discussion

### Identification of transcriptional units within the *cwps* gene cluster

The conserved, 5'-positioned region of the *cwps* cluster was proposed to encode the biosynthetic abilities for the production of the rhamnan component of the CWPS, whereas the more variable 3'-located region was proposed to encode for the biosynthesis of the PSP component (11, 15). Furthermore, the two chains are believed to be produced independently of each other because PSP-negative variants retain the rhamnan layer in their cell envelope (15). To identify potential promoter-containing regions within the *cwps* cluster in *L. lactis* NZ9000, eight intergenic regions present within this cluster (Fig. S2) were individually cloned upstream of the promoterless *lacZ* gene located on the pPTPL vector. When  $\beta$ -gal activity was detected, the presence of a promoter sequence in the cloned region was further validated by means of primer-extension analysis (Fig. S2). In this way, three transcription start sites (TSSs) were identified: 28 nucleotides upstream of the annotated translation start site of *rmlA* (for *NZProm1*), 60 nucleotides upstream of the annotated translational start site of *wpsA* (for *NZProm2*), and 94 nucleotides upstream of the annotated translation start site of *wpsH* (for *NZProm3*) (Fig. 1A). Based on the TSSs for *rmlA*, *wpsA*, and *wpsH*, corresponding –10 and –35 hexamers were identified by visual scrutiny (Fig. 2A). The identified –10 regions of the *L. lactis* NZ9000 *cwps* gene cluster closely resemble the conserved motif sequence of the –10 regions (TATAAT) in the MG1363 transcriptome, whereas the –35 hexamers do not show significant homology to the conserved motif (TTGACA) (21). The relative strength of each of the promoter-containing regions identified above was measured as specific  $\beta$ -gal activity and assessed at three different time points during growth (Fig. 2B). From the obtained results, it is clear that *NZProm1* consistently provided the highest level of expression followed by *NZProm2*, whereas *NZProm3* exhibited barely measurable  $\beta$ -gal activity. Notably, these results are consistent with previous work on the *L. lactis* MG1363 whole-genome transcriptome that identified two of these regions



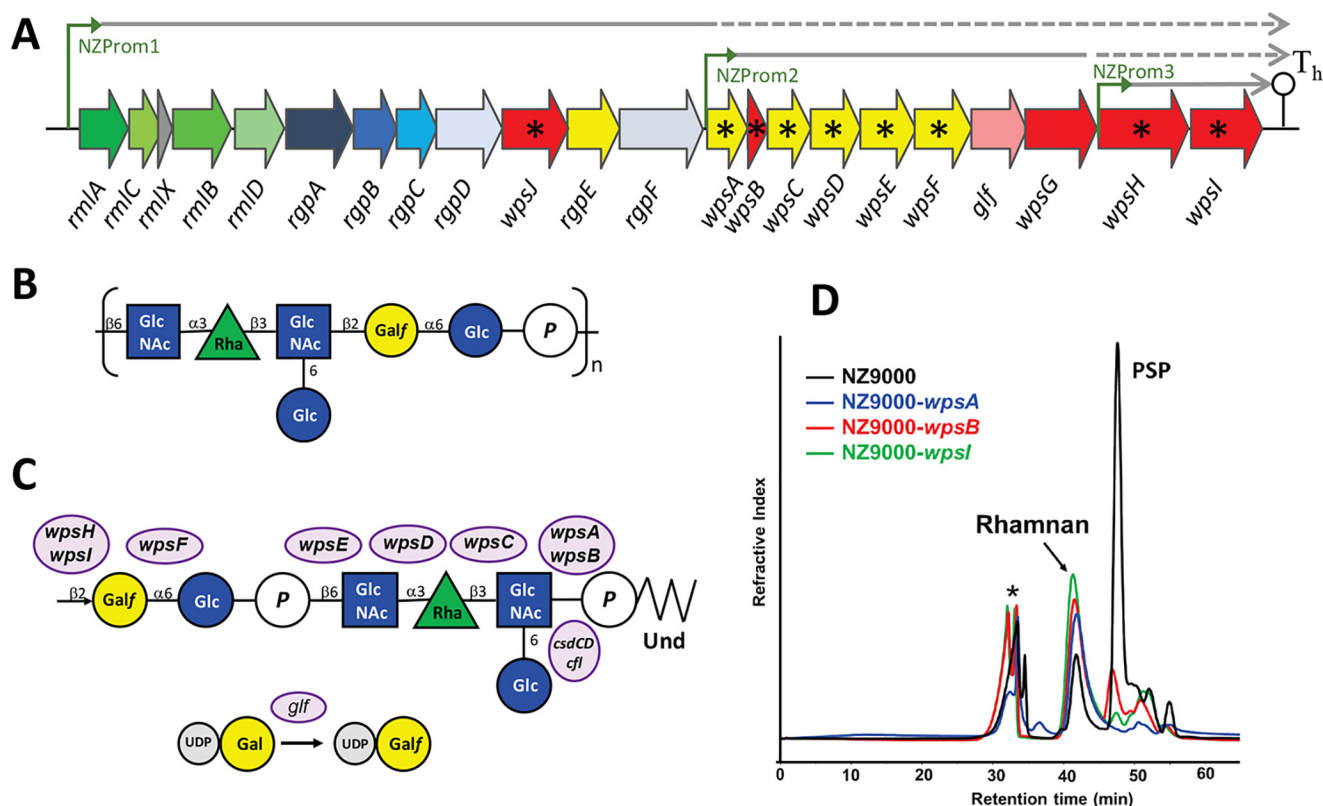


**Figure 1.** A, schematic representation of the *L. lactis* NZ9000 *cwps* gene cluster encoding the enzymatic machinery for rhamnan and PSP biosyntheses. Genes with successfully introduced nonsense mutations are indicated with an asterisk. The three identified transcriptional units and corresponding mapped promoters (NZProm1, NZProm2, and NZProm3) are indicated.  $T_h$ , potential terminator. Predicted functions of each encoded protein are listed in Table 1. Green, dTDP-Rha synthesis; blue, rhamnan synthesis; red, membrane proteins; yellow, glycosyltransferases. B, structure of the polymeric PSP from *L. lactis* NZ9000 as previously established by NMR analysis (13). C, upper part of image, predicted structure of the UndP-linked PSP subunit intermediate of *L. lactis* NZ9000 and genes proposed to be involved in the synthesis of each bond. Genes involved in Glc side-chain addition (*csdCD* and *cfl*) are located outside the *cwps* cluster. Lower part of image, formation of UDP-Galf for incorporation in the PSP repeat unit by UDP-galactofuranose mutase Glf. D, SEC-HPLC analyses of CWPS allowing separation of rhamnan and PSP oligosaccharides extracted from *L. lactis* NZ9000 and three derivative mutants. An asterisk indicates nonpolysaccharidic compounds.

(NZProm1 and NZProm2) as containing potential TSSs within the gene cluster (21). Additionally, the activity of these promoters appears to be growth phase-independent as it remains constant for all time points tested (Fig. 2B). These results indicate that CWPS biosynthesis is not regulated at the transcriptional level during growth under laboratory conditions. Further assessment of mRNA by means of reverse transcription (RT)-PCR indicated the occurrence of transcriptional read-through within the *cwps* gene cluster (Fig. S3).

In conclusion, we propose the presence of three transcriptional units (TUs) within the *cwps* gene cluster,  $TU_{rha}$  under the control of NZProm1,  $TU_{psp}$  under the control of NZProm2, and  $TU_{pol}$  under the control of NZProm3 (Fig. 1A). The transcriptional organization thus aligns with the previously hypothesized functional organization of the gene cluster.

#### Identification of protein candidates for PSP biosynthesis encoded in the *cwps* gene cluster

Regarding rhamnan biosynthesis, we have previously proposed a model based on an ABC transporter-dependent pathway, entailing intracellular polymerization of rhamnan before export at the outer side of the cytoplasmic membrane (15). This model involves nine genes located in the more constant part of the *cwps* cluster, with the four genes predicted to be involved in

dTDP-Rha precursor (*rmlA*, *rmlB*, *rmlC*, and *rmlD*), the three genes encoding putative rhamnosyltransferases (*rgpA*, *rgpB*, and *rgpF*), and the two genes encoding an ABC transporter (*rgpC* and *rgpD*) (Fig. 1A). In addition, we have shown that a *tagO* homolog (*lhz\_010205*), encoding a putative phosphoglycosyltransferase (PGT) that belongs to the WecA family and located outside of the *cwps* gene cluster in *L. lactis* NZ9000, plays a role in rhamnan synthesis presumably as the initial transferase. Also, we obtained proof that LcpA is most likely the major LCP protein involved in rhamnan attachment to peptidoglycan.

In our previous studies (11, 13, 15), we have gathered several lines of evidence that the more variable 3'-located region of the *cwps* cluster is involved in PSP biosynthesis. This region, which is under the control of NZProm2, contains five genes encoding putative glycosyltransferases, one encoding a putative UDP-galactopyranose mutase, and four encoding membrane proteins (Fig. 1A). Of note, three other genes, *rmlX*, *rgpE*, and *wpsJ*, located in the more conserved part, do not yet have assigned functions. Because PSP is a heteropolysaccharide composed of repeating phospho-hexasaccharide subunits (Fig. 1B) (13) and due to the presence of a putative flippase-encoding gene (*wpsG*) (Table 1) in the variable part of the *cwps* gene cluster, we sug-

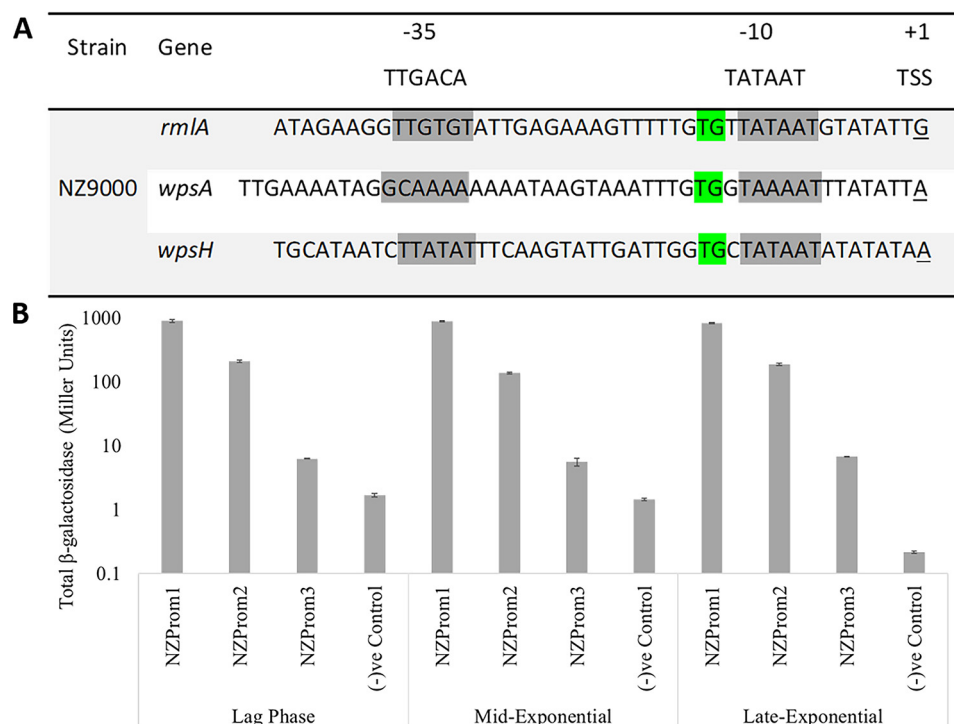


**Figure 2.** A, summary of the identified promoter-containing regions along with the transcription start sites for each gene. Each of the  $-10$  and  $-35$  hexamer sites was identified based on nucleotide distance from the TSS. The conserved  $-10$  and  $-35$  hexamers of MG1363 are indicated in *bold* (21). Highlighted in green is the dinucleotide TG motif found commonly upstream of the lactic acid bacteria  $-10$  promoter region, which has previously been shown to enhance promoter activity and is commonly found upstream of the  $-10$  motif in lactic acid bacteria. B, specific  $\beta$ -gal activity of *L. lactis* strains NZ9000 containing either pPTPL::NZProm1, pPTPL::NZProm2, or pPTPL::NZProm3 and control strain *L. lactis* NZ9000 pPTPL measured during the lag, mid-exponential, and late-exponential phases of growth. (–)ve, negative. Error bars represent S.D.

**Table 1**  
Proteins encoded in the *L. lactis* NZ9000 *cwps* locus and their predicted functions

Locus tag	Gene name	Predicted function of the encoded protein <sup>a,b</sup>
<i>llnz_1075</i>	<i>rmlA</i>	Glucose-1-phosphate thymidyltransferase, biosynthesis of dTDP-Rha precursor
<i>llnz_1080</i>	<i>rmlC</i>	dTDP-4-dehydrorhamnose 3,5-epimerase, biosynthesis of dTDP-Rha precursor
<i>llnz_1085</i>	<i>rmlX</i>	Hypothetical protein
<i>llnz_1090</i>	<i>rmlB</i>	dTDP-glucose 4,6-dehydratase, biosynthesis of dTDP-Rha precursor
<i>llnz_1095</i>	<i>rmlD</i>	dTDP-4-dehydrorhamnose reductase, biosynthesis of dTDP-Rha precursor
<i>llnz_1100</i>	<i>rgpA</i>	Glycosyltransferase family 4 (GT4) protein, putative $\alpha$ -D-GlcNAc $\alpha$ -1,2-L-rhamnosyltransferase, rhamnan chain elongation
<i>llnz_1105</i>	<i>rgpB</i>	Glycosyltransferase family 2 (GT2) protein, putative $\alpha$ -L-Rha $\alpha$ -1,3-L-rhamnosyltransferase, rhamnan chain elongation
<i>llnz_1110</i>	<i>rgpC</i>	ABC transporter permease, 6 TMHs, export of rhamnan
<i>llnz_1115</i>	<i>rgpD</i>	ABC transporter ATP-binding protein, export of rhamnan
<i>llnz_1120</i>	<i>wpsJ</i>	Membrane protein with a DUF2142 domain, 9 TMHs
		Structural similarity found with glycosyltransferases with a GT-C fold
<i>llnz_1125</i>	<i>rgpE</i>	Glycosyltransferase family 2 (GT2) protein
<i>llnz_1130</i>	<i>rgpF</i>	Putative $\alpha$ -L-Rha $\alpha$ -1,2-L-rhamnosyltransferase, rhamnan chain elongation
<i>llnz_1135</i>	<i>wpsA</i>	43% sequence identity with <i>S. pyogenes</i> GacI, a UDP-GlcNAc:Und-P GlcNAc-transferase
<i>llnz_1140</i>	<i>wpsB</i>	Hypothetical protein, 3 TMHs, 33% sequence identity with <i>S. pyogenes</i> GacJ, activator of GacI
<i>llnz_1145</i>	<i>wpsC</i>	Glycosyltransferase family 2 (GT2) protein
<i>llnz_1150</i>	<i>wpsD</i>	Glycosyltransferase family 2 (GT2) protein
<i>llnz_1155</i>	<i>wpsE</i>	Hypothetical protein with a Stealth domain (PF11380)
<i>llnz_1160</i>	<i>wpsF</i>	UDP-galactofuranose transferase
<i>llnz_1165</i>	<i>glfI</i>	UDP-galactopyranose mutase
<i>llnz_1170</i>	<i>wpsG</i>	Putative O-antigen transporter, 13 TMHs, 24% sequence similarity with <i>E. coli</i> Wzx flippases
<i>llnz_1175</i>	<i>wpsH</i>	Membrane protein, 2 TMHs
<i>llnz_1180</i>	<i>wpsI</i>	Membrane protein with a DUF2142 domain, 9 TMHs, structural similarity found with glycosyltransferases with a GT-C fold

<sup>a</sup> According to Integrated Microbial Genomes and Microbiomes System v.5.0 annotation, structural similarity prediction by HHpred analysis and sequence identity search by BlastP. *rgp* gene functions were deduced from *Streptococcus mutans* homologs (46).

<sup>b</sup> TMHs as predicted by TMHMM Server v.2.0.

gest that PSP subunits are synthesized in the cytoplasm on a lipid carrier and further exported, polymerized, and ligated to rhamnan chains. The expected steps of the PSP biosynthesis would thus be as follows: (i) initiation of PSP subunit synthesis onto a lipid carrier, presumably Und-P, at the inner face of the cytoplasmic membrane; (ii) elongation of the PSP subunit on the lipid carrier by dedicated glycosyltransferases in the cyto-

plasm; (iii) export of the lipid-linked subunit at the outer face of the membrane; and (iv) polymerization and anchoring onto rhamnan. We performed an in-depth bioinformatics analysis of the sequences of proteins encoded by the *cwps* gene cluster (Table 1), and we propose below possible candidates for the different steps required for PSP biosynthesis and anchoring to rhamnan.

## Initiation of PSP repeat unit synthesis

Initiation of glycan chain synthesis in bacteria is usually performed by PGTs that catalyze the transfer of a phosphosugar from a UDP-sugar to the lipid carrier Und-P, leading to a Und-diphosphate-sugar precursor (22). According to sequence analysis, no typical PGT belonging to either the WecA or WbaP family is encoded within the *cwps* cluster (Table 1). As mentioned above, we have previously identified a putative PGT belonging to the WecA family encoded by a gene (named *tagO*) outside of the *cwps* gene cluster in *L. lactis* NZ9000, which appears to be the initial transferase involved in rhamnan synthesis (15). This enzyme is expected to catalyze the transfer of GlcNAc-P from UDP-GlcNAc to Und-P, leading to Und-P-P-GlcNAc precursor. Because no other PGT candidate could be identified in the *L. lactis* NZ9000 genome, TagO could also constitute a putative candidate for PSP subunit synthesis initiation.

However, synthesis of oligosaccharidic chains was also reported to be initiated by formation of polyprenyl monophosphate-sugar rather than the more widely spread polyprenyl diphosphate-sugar in rare cases such as the synthesis of the glycan part of glycoproteins in Archaea (23). Interestingly, sequence and structure homology analyses predict that the first gene of the transcriptional unit under the control of NZProm2, *wpsA*, encodes a glycosyltransferase able to catalyze the synthesis of Und-monophosphate-monosaccharide. Indeed, WpsA is a putative glycosyltransferase (245 AA) (with a short N-terminal hydrophobic segment but no clear transmembrane helix (TMH) or signal peptide) belonging to the GT-A family (glycosyltransferase, family 2). WpsA exhibits 43% amino acid identity with the *Streptococcus pyogenes* protein GacI that was biochemically characterized as a UDP-GlcNAc:Und-P GlcNAc-transferase (24). In *S. pyogenes*, GacI is proposed to synthesize Und-P-GlcNAc at the cytoplasmic side of the membrane, which after transport to the extracellular side is a donor substrate for an integral membrane glycosyltransferase with a GT-C fold (GacL) that adds GlcNAc on the *S. pyogenes* polyrhamnose cell-wall polysaccharide. In addition, the gene located downstream of *wpsA*, *wpsB*, encodes a small membrane protein of 117 amino acids with three TMH segments and that exhibits 33% sequence identity and similar topology with *S. pyogenes* GacJ that was shown to stimulate the catalytic activity of GacI (24). Like in *S. pyogenes*, it can be envisaged that the two proteins, WpsA and WpsB, are involved in rhamnan decoration with GlcNAc, although only traces of GlcNAc were previously detected associated to purified lactococcal rhamnan (15). Alternatively, we speculate that WpsA and WpsB could initiate the biosynthesis of the PSP subunit by generating an Und-monophosphate-sugar intermediate rather than the classically found Und-diphosphate-sugar intermediate generated by PGT enzymes. This hypothesis is also supported by the location of the *wpsA* and *wpsB* genes in the transcriptional unit associated to PSP biosynthesis (Fig. 1A).

## Elongation of the PSP repeat unit

Downstream of *wpsA* and *wpsB*, the four genes *wpsC*, *-D*, *-E*, and *-F* encode putative glycosyltransferases, which could be

involved in the iterative synthesis of the PSP repeat unit. The four glycosyltransferases WpsC, *-D*, *-E*, and *-F* are devoid of putative transmembrane segments, indicative of a probable cytoplasmic location, which thus supports the notion of intracellular synthesis of the PSP subunit. The *wpsC* and *wpsD* genes encode two glycosyltransferases (with 264 and 330 AA, respectively), belonging to family 2 (Pfam PF00535) with a GT-A-type fold, whose substrate and product cannot be predicted from sequence analysis. The gene *wpsE* encodes a protein (332 AA) with a Stealth\_CR2 (PF11380) domain (positions 40–141), present in D-hexose 1-phosphate transferases, which generate interglycosidic phosphate diester linkages (47). WpsE could thus catalyze Glc-P addition in the PSP subunit. The *wpsF* gene encodes a glycosyltransferase (344 AA) with a putative galactofuranose transferase activity (domain PIRSF007023, *UDP-Galf\_galf\_transf*). WpsF could thus be involved in Galf addition in the PSP subunit. The gene *glf* encodes a putative UDP-galactopyranose mutase, an enzyme catalyzing the conversion of UDP- $\alpha$ -D-galactopyranose to UDP- $\alpha$ -D-galactofuranose, which could provide the nucleotide precursor substrate for incorporation of Galf into the PSP subunits by WpsF. Thus, these four enzymes, WpsC, *-D*, *-E*, and *-F*, in addition to the initial sugar transferase would be able to synthesize a pentasaccharide containing a phosphate on the lipid carrier UndP as hypothesized in Fig. 1C. Regarding the side-chain Glc present in the PSP subunit of NZ9000, we have recently found that the genetic determinants contributing to the addition of this sugar on PSP subunits are located outside of the *cwps* gene cluster.<sup>6</sup>

## Export of the PSP subunits

The *wpsG* gene encodes an integral membrane protein containing 13 predicted TMHs. Blast analysis revealed 24% sequence identity with *Escherichia coli* flippase Wzx involved in O-antigen synthesis, more precisely involved in flipping the subunit linked to Und-PP outside of the cytoplasmic membrane. In addition, HHpred analysis of WpsG revealed significant structural similarity to lipid II flippase MurJ (probability, 100%; E-value,  $5.7e^{-36}$ ; Protein Data Bank (PDB) structure 5T77) that catalyzes the translocation of the lipid-linked precursor of peptidoglycan across the lipid membrane. Despite these similarities with flippases acting on Und-PP-linked substrates and because no other putative flippase is encoded in the *cwps* cluster, we hypothesize that WpsG represents the flippase that transfers Und-P-linked PSP subunit to the extracellular face of the bacterial membrane.

## Polymerization of PSP subunits

The two next genes, *wpsH* and *wpsI*, encode two membrane proteins. Notably, these two genes are highly conserved among strains classified as C type based on the *cwps* cluster analysis (11), including in particular the three strains with a PSP characterized as a polymeric chain made of repeating units of phospho-oligosaccharide. In contrast, these genes are absent in type A (UC509.9) and type B (IL1403) where the variable part of CWPS constitutes short oligosaccharide chains without any

<sup>6</sup> I. Theodorou, P. Courtin, I. Sadovskaya, S. Palussière, F. Fenaille, J. Mahony, M.-P. Chapot-Chartier and D. van Sinderen, unpublished data.



repetition (16, 17) (Fig. S1). These observations support the hypothesized role of the two membrane proteins in PSP subunit polymerization.

WpsI is an integral membrane protein with nine predicted TMHs. No sequence homology was found with known Wzy polymerases involved in polymerization of oligosaccharide subunits in the Wzx/Wzy-dependent pathway for (lipo)polysaccharide synthesis. WpsI contains a DUF2142 (PF09913) domain with no known function but that belongs to the GT-C clan containing glycosyltransferases with 8–13 predicted TMHs and that are dependent on polyprenyl phosphate-linked sugars (8, 25). In particular, WpsI contains the typical modified catalytic DXD motif (<sup>63</sup>EPD<sup>65</sup>) located in the first predicted large extracellular loop located after the first TMH segment (Fig. S5). HHpred analysis also predicts structural similarity to several membrane-associated glycosyltransferases known to possess a GT-C fold, including 4-amino-4-deoxy-L-arabinose (L-Ara4N) transferase (ArnT) (probability, 99.1%; E-value,  $1.4 \times 10^{-9}$ ; PDB structure 5EZM\_A) and the archaeal oligosaccharyltransferase AglB (probability, 98.55%; E-value,  $8.3 \times 10^{-7}$ ; PDB structure 3WAJ\_A), which catalyzes the transfer of oligosaccharide chains from lipid-oligosaccharide precursors to Asn residues in proteins. Notably, most of the known GT-C enzymes utilize lipid-monophosphate-sugar as activated sugar donor and transfer the sugar on various glycan acceptors, and they can be part of three-component modifying systems (8). Therefore, we propose that WpsI is responsible for the transfer of the PSP subunit from a lipid precursor (Und-P subunit) to an acceptor that could be either another PSP subunit or, alternatively, rhamnan. The fact that *wpsI* is absent in the *cwps* locus of strains that do not produce polymeric PSP supports the notion that WpsI is involved in the polymerization of PSP by transfer of the PSP subunit linked to a lipid carrier onto another acceptor PSP subunit.

WpsH is also a membrane protein with two predicted TMHs close to the N and C termini, respectively, and a large loop outside the cytoplasmic membrane (Fig. S5). This topological organization resembles that of Wzz proteins that have been proposed to be copolymerases regulating (lipo)polysaccharide chain length in the Wzy-dependent pathway (26). However, WpsH does not exhibit sequence identity with *E. coli* Wzz proteins and exhibits no significant structural similarity with members of the family (as searched by HHpred analysis). Nevertheless, because of the conserved topography with Wzz, we speculate that WpsH plays a regulatory role in PSP polymerization by WpsI as a copolymerase. The presence of promoter *NZProm3* (Fig. 1A) upstream of *wpsH* and *wpsI* further supports a functional link between the two genes.

#### Attachment of PSP to rhamnan

From our previous results (15), we gathered evidence that rhamnan is anchored to peptidoglycan, whereas PSP may be attached to rhamnan, thereby constituting a large heteropolysaccharide in the cell wall. In the more conserved part of the *cwps* gene cluster, the *wpsJ* gene encoding a putative integral membrane protein (463 AA) with nine TMHs is conserved among *L. lactis* genomes but exhibits sequence variability. WpsJ does not exhibit significant sequence identity with any

protein with known function but contains a DUF2142 (PF09913, IPR018674) domain that belongs to the GT-C clan containing glycosyltransferases with 8–13 predicted TMH segments and that are dependent on polyprenyl phosphate-linked sugars. Notably, it contains a modified catalytic DXD motif (<sup>43</sup>EPD<sup>45</sup>) located in the first predicted extracellular loop of the protein (Fig. S5). It exhibits 35% sequence identity with WpsI in its N-terminal part with conserved residues around the EPD motif found in both proteins. Similarly to WpsI, HHpred analysis predicts structural similarity with several membrane glycosyltransferases that are typical enzymes with a GT-C fold, such as ArnT (probability, 99.01%; E-value,  $4.4 \times 10^{-9}$ ; PDB structure 5EZM\_A). Therefore, we hypothesize that WpsJ, being encoded by *wpsJ* located in the more conserved part of the *cwps* gene cluster among the genes encoding rhamnan biosynthesis, constitutes the transferase involved in attaching PSP to the rhamnan chain.

Two genes are then left without proposed function in the *cwps* cluster. The *rgpE* gene located in the more conserved part is predicted to encode a family 2 glycosyltransferase without a TMH segment, and it is present in strains with type A, B and C CWSPs (12). We suggest that RgpE is involved in rhamnan chain termination, thus regulating rhamnan length, by adding a sugar at the nonreducing end as proposed previously for other PSs synthesized by an ABC-transporter pathway (6). Our previously reported mass spectrometry (MS) analysis of rhamnan from *L. lactis* MG1363 and the absence of terminal Rha have indeed suggested the presence of a sugar (GlcNAc or Glc) at the nonreducing end of the rhamnan chain (15). The second gene without assigned function, *rmlX*, encodes a small protein exhibiting no sequence homology with protein of known function, which we presume to be implicated in the dTDP-Rha precursor synthesis.

#### Construction of NZ9000 derivatives carrying mutations in the *cwps* gene cluster

To perform a functional analysis of individual genes of the *L. lactis* NZ9000 *cwps* gene cluster, knockout mutants were created by a CRISPR recombineering approach. With the exception of the first five genes (*rmlA*, *rmlC*, *rmlX*, *rmlB*, and *rmlD*) in the cluster that are presumed to be part of the *rml* pathway for the production of the precursor molecule for rhamnose (*i.e.* dTDP-Rha) and essential for bacterial growth (27), gene knockout mutants were attempted for all other genes of the *cwps* cluster. Due to the nature of these mutations and their effect on strain fitness, “classical” recombineering was not successful in isolating and maintaining the majority of desired mutations in the *cwps* gene cluster. Instead, CRISPR–Cas9-assisted recombineering was used to facilitate the construction and stable maintenance of these gene knockout mutants (Fig. S3). Nevertheless, it appeared impossible to knock out eight of the 17 targeted genes, the majority of which were located within the 5' conserved region of the gene cluster. Nonetheless, knockout mutants of the majority of the genes located in the more variable 3'-located end of the cluster were obtained with the exception of *wpsH* and *glf*, which encode a putative flippase and UDP-Gal mutase, respectively. In contrast, in the more conserved 5' region, only *wpsJ* could be inactivated (Fig. 1A and Table S1).

## CWPS analysis of the mutant derivatives

CWPS of the obtained mutants was extracted and analyzed. For this purpose, cell walls were prepared from the mutant strains, and CWPS was extracted by hydrofluoric acid (HF) treatment. Regarding the control WT *L. lactis* NZ9000, HF extract contains rhamnan and oligosaccharides derived from PSP by cleavage of the phosphodiester bonds inside the PSP chain, which can be separated as two major peaks when subjected to SEC–HPLC analysis as described previously (15) (Fig. 1B). The SEC–HPLC profile of the CWPS extracted from the nine mutants revealed first that all mutants are able to synthesize rhamnan (Fig. 1D and data not shown). Notably, inactivation of *wpsJ*, located in the more conserved part of the *cwps* gene cluster, did not prevent the synthesis of rhamnan (data not shown). In contrast, all obtained mutants were severely affected in PSP synthesis. Only mutant NZ9000-*wpsB* exhibited a SEC–HPLC profile with a clearly detectable peak of PSP oligosaccharides but at a very substantially reduced level relative to rhamnan when compared with WT NZ9000 (Fig. 1D).

Despite the apparent absence or very low amounts of PSP in the mutants according to the SEC–HPLC profile, we reasoned that such mutants may still be able to synthesize residual amounts of oligosaccharides originating from aborted synthesis of the PSP subunit due to the mutation, which may be detectable by a highly sensitive technique such as MS. Thus, we employed MALDI-TOF MS to analyze the content of the fractions collected by SEC–HPLC with the elution times corresponding to WT PSP peak for each mutant. Regarding WT NZ9000, the spectrum obtained on PSP oligosaccharides (Fig. 3) reveals main peaks at  $m/z$  1079.41 assigned to the hexasaccharide resulting from depolymerization of PSP chain by cleavage at phosphodiester bonds and at  $m/z$  917.23 assigned to the pentasaccharide obtained by partial cleavage of the hexasaccharide by HF after GalF as identified previously by nuclear magnetic resonance (NMR) analysis (Fig. 1B) (13). The spectra obtained for the various mutants (presented in Fig. 3) show different patterns that correspond to (i) a spectrum similar to that of WT NZ9000 (mutant *wpsB*), (ii) a spectrum with  $m/z$  values lower than expected for the complete hexasaccharide PSP subunit (mutants *wpsD*, *wpsE*, *wpsF*, *wpsH*, and *wpsI*), and (iii) the absence of chemical species detected (mutants *wpsA*, *wpsC*, and *wpsJ*).

In mutant NZ9000-*wpsA*, no PSP-derived oligosaccharide was detectable by MALDI-TOF MS, whereas in the NZ9000-*wpsB* mutant, a spectrum similar to that of WT NZ9000 was obtained, in agreement with the SEC–HPLC profile showing the presence of PSP albeit at a much reduced level when compared with WT (Figs. 1D and 3). These results indicate that both WpsA and WpsB play a role in PSP synthesis but that WpsA is absolutely required for PSP synthesis, whereas WpsB is not. They support the role hypothesized above for WpsA/WpsB in the initiation of PSP synthesis. According to its predicted enzymatic activity of UDP-GlcNAc:Und-P GlcNAc-transferase, WpsA would thus catalyze the first step of PSP subunit assembly and initiate synthesis by transferring GlcNAc from UDP-GlcNAc to Und-P, and WpsB would stimulate WpsA activity. The results of CWPS analysis are consistent

with this hypothesis because inactivation of *wpsA* is thus expected to totally abrogate PSP synthesis, whereas inactivation of *wpsB* is expected to only decrease the efficiency of PSP initiation, thus lowering the final amount of PSP.

The MALDI-TOF MS spectra obtained for mutants of glycosyltransferase-encoding genes *wpsD*, *wpsE*, and *wpsF* exhibit peaks with  $m/z$  values lower than that detected in the WT spectrum (Fig. 3). The obtained  $m/z$  values were found to support the predicted model for PSP subunit synthesis presented in Fig. 1C, with WpsC and WpsD adding successively Rha and GlcNAc, WpsE adding Glc-P, and WpsF adding GalF, assuming cleavage of phosphodiester bonds inside the subunit due to HF extraction to assign structures to the different peaks (Fig. 3). Of note, the deduced structures contain (at least partially) the side-chain Glc, which we have found to be added by a three-component glucosylation system located outside the *cwps* cluster.<sup>6</sup> Regarding NZ9000-*wpsC*, the absence of any detected signal is presumably linked to the small size of the residual PSP, if any, expected to be a disaccharide (or only GlcNAc).

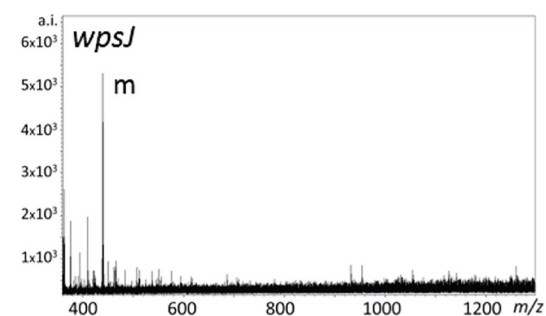
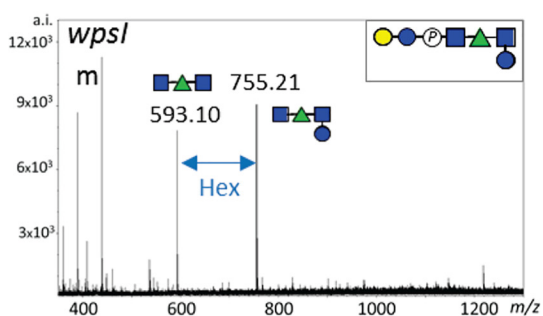
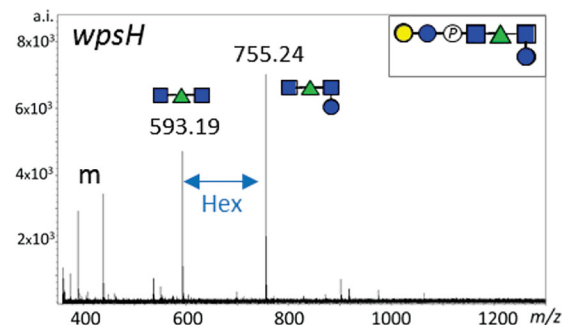
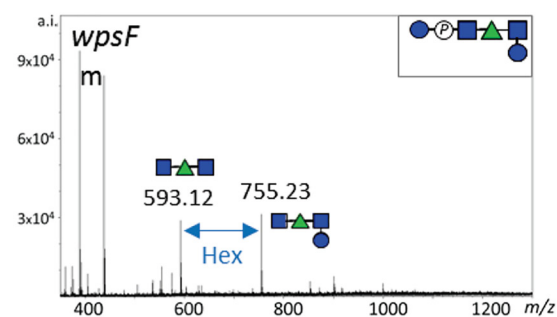
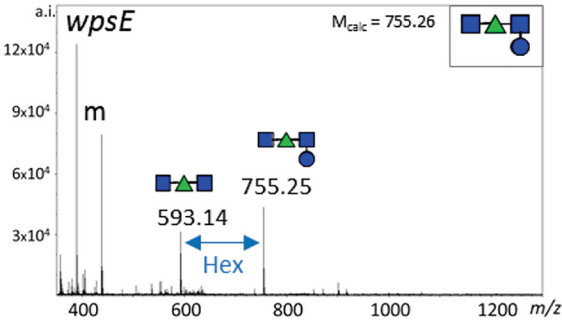
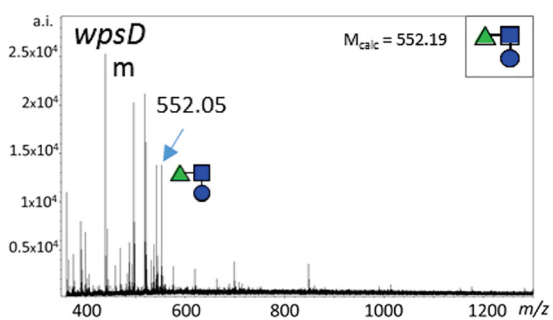
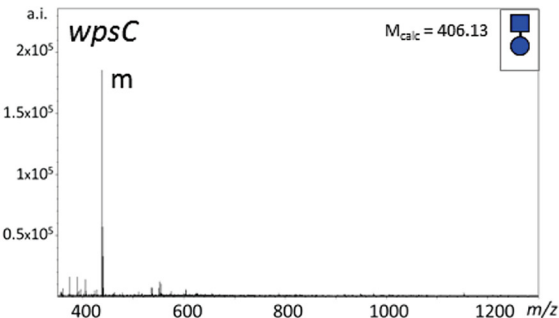
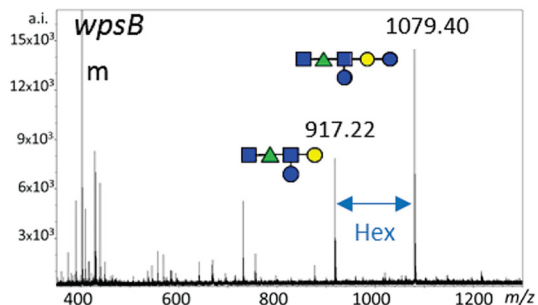
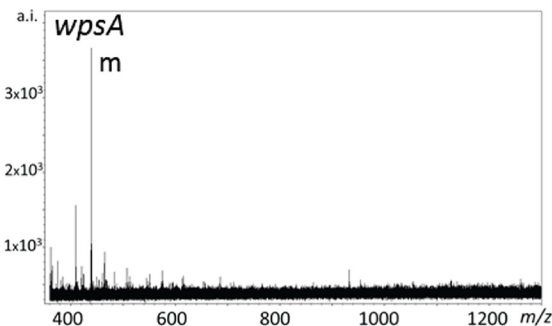
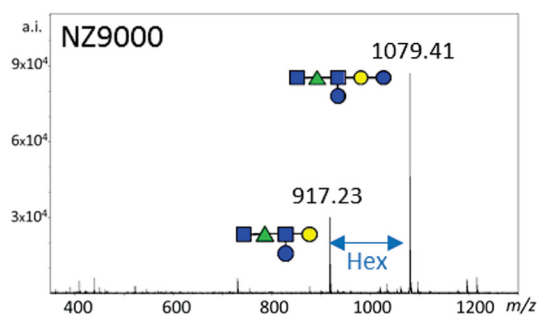
The MS spectra from the two mutants NZ9000-*wpsH* and -*wpsI* also differ from the WT spectrum and revealed peaks with  $m/z$  values of 755.21 and 593.10 (Fig. 3), consistent with structures corresponding to single PSP subunit (as represented in Fig. 1C) cleaved by HF at the level of the phosphodiester bond. Notably, the peaks corresponding to polymeric chains found in the WT spectrum were not detected, thus supporting impairment of PSP polymerization in these two mutants. These data are in agreement with the proposed role of WpsH and WpsI in PSP polymerization.

Regarding the NZ9000-*wpsJ* mutant, CWPS analysis by SEC–HPLC showed the presence of the rhamnan peak but the absence of the PSP peak (profile similar to NZ9000-*wpsA*) (data not shown). In addition, no signal could be detected by MS analysis of the fractions eluting at the same retention time as the WT PSP peak (Fig. 3). These results indicate that *wpsJ*, located in the more conserved part of the *cwps* cluster, is essential for PSP assembly in the cell wall. Although they do not definitively prove the role of WpsJ, our results are consistent with the hypothesized role of WpsJ in the transfer of PSP onto rhamnan, which would be a necessary step for PSP to be extracted by HF after purification of the cell walls as described under “Experimental procedures.”

## Growth and morphology of the *cwps* mutant derivatives

All nine *cwps* mutants presented with an impaired growth phenotype compared with the control strains in liquid broth conditions, whereas they exhibited a reduced colony size on solid agar plates. In addition, the mutants also exhibited an increased level of sedimentation in liquid culture compared with the control strains, as reported for the previously characterized PSP-negative *L. lactis* VES5751 spontaneous mutant (13). A few selected mutants were then examined by transmission EM (TEM). We have previously observed that PSP forms an outer pellicle in *L. lactis* MG1363 (and NZ9000) that appears as a dark electron-dense layer on TEM micrographs (13). As shown in Fig. 4 and in contrast to NZ9000, the mutants NZ9000-*wpsA*, NZ9000-*wpsH*, and NZ9000-*wpsJ* are devoid of any outer dark layer. These observations corroborate our bio-





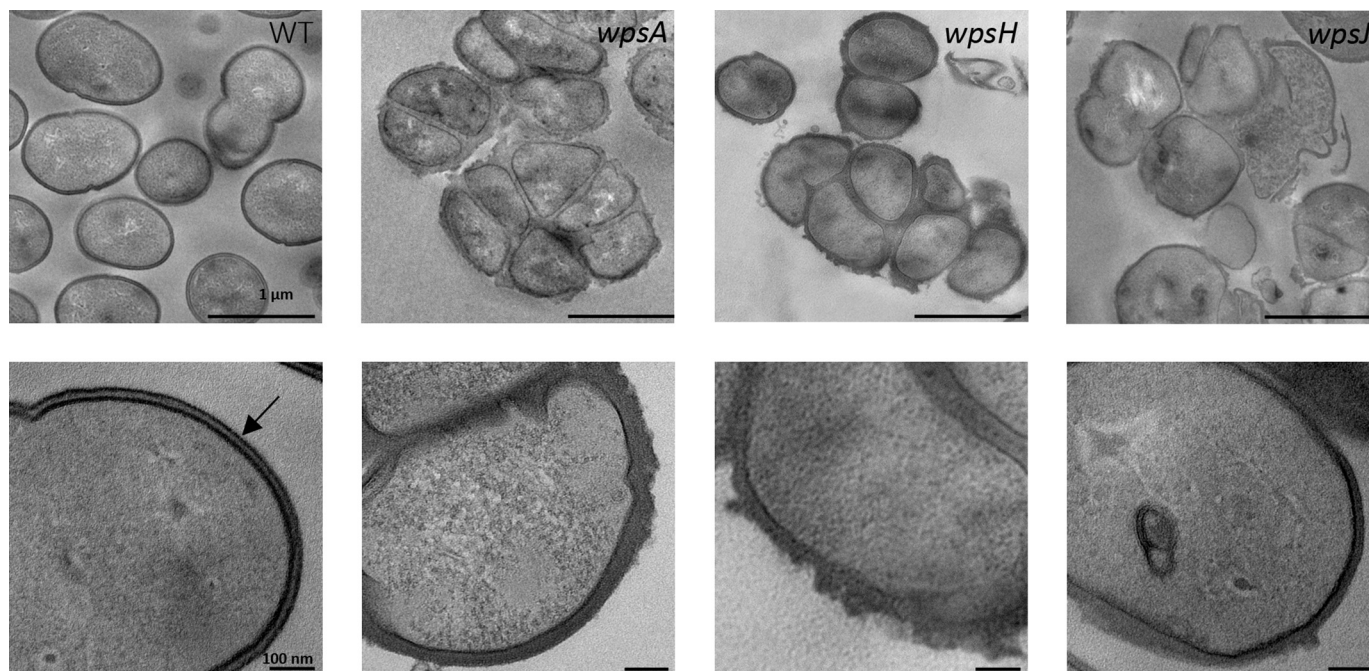


**Figure 4. TEM micrographs of *L. lactis* NZ9000 WT and derivative knockout mutants NZ9000-*wpsA*, NZ9000-*wpsH*, and NZ9000-*wpsJ*.** The arrow indicates the outer dark layer surrounding WT cells of *L. lactis* NZ9000 and attributed previously to the presence of the pellicle (PSP). This layer is absent in cells of *wpsA*, *wpsH*, and *wpsJ* mutants.

chemical data presented above, indicating the absence of PSP chains in the cell wall of these mutants. We also observed severe alterations of shape and impairment of cell division in the mutants devoid of PSP chains, *i.e.* mutants NZ9000-*wpsA*, -*wpsH*, and -*wpsJ*, suggesting that intact PSP is required for proper cell-wall assembly in *L. lactis*.

#### Bacteriophage sensitivity of cwps mutant derivatives

PSP-negative mutants have been previously characterized as resistant to bacteriophages infecting *L. lactis* (11, 13). Moreover, several phage receptor-binding proteins were found to bind the surface-exposed PSP (28, 29). All *cwps* gene knockout mutants were thus assayed for their sensitivity against phages that are able to infect the WT *L. lactis* NZ9000 and known to use CWPS as receptors (Table 2). All three phages assayed (jj50, p2, and sk1) were unable to infect seven of the nine CWPS mutant strains, presumably due to their PSP-deficient phenotype. Interestingly, they were still able to infect the NZ9000-*wpsB* mutant that is, according to our CWPS analysis, capable of synthesizing polymeric PSP, albeit at a reduced level compared with WT. Although it appears that phages p2 and sk1 are also capable of infecting NZ9000-*wpsI* in which we did not detect polymeric PSP, their infection efficiency remains significantly lower than that observed in the cases of WT NZ9000 and NZ9000-*wpsB*.

Moreover, we successfully isolated eight escape mutants of phage sk1 (Table S1) against the spontaneous PSP-deficient mutant *L. lactis* VES5751 (*wpsH* mutant). Their infectivity profiles against the CWPS knockout mutants constructed in this study were also investigated and could be classified into two profiles (Table 2). All these mutants were still able to infect WT NZ9000 and NZ9000-*wpsB* mutant, which both synthesize PSP chains. In addition and interestingly, the escape mutants could infect a subset of the CWPS mutants, specifically the mutants that we predicted to be able to synthesize remnants of the PSP corresponding to a single complete PSP repeat unit or a truncated one of sufficient size (at least three or four sugars for each group, respectively, with or without Glc side chain). In contrast, CWPS mutants in which no PSP fragments could be detected by MS (*i.e.* mutants NZ9000-*wpsJ*, -*wpsA*, and -*wpsC*) or were presumed to produce small amounts of a very shortened PSP subunit (disaccharide with or without side-chain Glc) (NZ9000-*wpsD*) remained completely resistant to the phage escape mutants.

Sequencing of the genomes of the sk1 phage derivatives revealed that each of the eight escape mutant phage had acquired between four and seven SNPs (Table S4), most of which are located within the baseplate-encoding region involved in phage adsorption to host surface PSP receptors.

**Figure 3. MALDI-TOF MS spectra of PSP fragments extracted by HF from cell walls of *L. lactis* NZ9000 and the nine constructed mutants.** *m/z* values correspond to  $[M + Na]^+$  adducts. *L. lactis* NZ9000 synthesizes polymeric PSP that is cleaved during HF extraction at the level of phosphodiester bonds, leading to hexasaccharide (calculated *m/z*  $[M + Na]^+$ , 1079.37), and partially also between Gal and Glc, leading to a pentasaccharide (calculated *m/z*  $[M + Na]^+$ , 917.32), as shown previously by NMR (13). A similar spectrum is found for *L. lactis* NZ9000-*wpsB*. For the remaining *wps* mutants, the expected structure of the (truncated) single PSP subunit deduced from our biosynthesis model, before HF cleavage of the phosphodiester bond, is represented in the right top corner of the spectrum. Similarly, figures within the spectrum indicate proposed PSP fragment structures based on *m/z* values. *m/z* values with a 162-mass-unit decrease are assigned to PSP fragments devoid of side-chain Glc. Hex, hexose; M, matrix; blue square, GlcNAc; green triangle, Rha; blue circle, Glc; yellow circle, Gal; P, phosphate. *a.i.*, absolute intensity;  $M_{calc}$ , calculated *m/z* of  $[M + Na]^+$  adducts.

**Table 2****Phage host range against *L. lactis* NZ9000 control strain as well as nine cwps gene mutant derivatives**

The tested phages include three WT 936 lytic phages commonly infecting *L. lactis* NZ9000 as well as eight escape mutant derivatives of phage sk1 isolated on *L. lactis* VES5751 (a *wpsH* spontaneous mutant).

Bacterial strain	Predicted PSP structure <sup>b</sup>	Bacteriophages <sup>a</sup>				
		Wild-type	Escape mutants			
		jj50	p2 sk1	MCC1 IT1 IT3	MCC5 MCC17 IT2 IT4 IT5	
WT NZ9000		✓	✓	✓	✓	
NZ9000- <i>wpsA</i>	-	✗	✗	✗	✗	
NZ9000- <i>wpsB</i>		✓	✓	✓	✓	
NZ9000- <i>wpsC</i>		✗	✗	✗	✗	
NZ9000- <i>wpsD</i>		✗	✗	✗	✗	
NZ9000- <i>wpsE</i>		✗	✗	✗	✓	
NZ9000- <i>wpsF</i>		✗	✗	✓	✓	
NZ9000- <i>wpsH</i>		✗	✗	✓	✓	
NZ9000- <i>wpsI</i>		✗	(✓)*	✓	✓	
NZ9000- <i>wpsJ</i>	-	✗	✗	✗	✗	

<sup>a</sup> ✓, phage infection; (✓)\*, observed infection efficiency significantly lower than infection of *L. lactis* NZ9000 WT and NZ9000-*wpsB*; ✗ = no infection.

<sup>b</sup> PSP structures as deduced from Maldi-ToF MS analysis (see Fig. 3). Blue square, GlcNAc; green triangle, Rha; blue circle, Glc; yellow circle, Gal; P, phosphosphate.

These results confirm that, in all phage escape mutants, the host recognition machinery had been adapted to bind to the remnant PSP fragments. Overall these results give further support to our biochemical data obtained on the constructed *wcps* mutants and the proposed model of subunit synthesis presented in Fig. 1C.

### Proposed model for the biosynthesis of *L. lactis* CWPS

From the bioinformatics analysis and from the phenotypic analysis of the constructed mutants, we deduced a complete biosynthesis pathway, presented in Fig. 5, for the complex cell-wall heteropolysaccharide of *L. lactis* NZ9000 comprising both rhamnan and PSP chains. In this model, we propose that the rhamnan chain and the PSP subunit are independently synthesized intracellularly on two different lipid-sugar intermediates and that assembly of the whole CWPS takes place outside the cytoplasmic membrane. The pathway proposed here for PSP biosynthesis and linkage to rhamnan can be envisioned as a novel variation on the theme of the three-component mechanism for bacterial cell-envelope glycoconjugate modification described previously (8). In the present case, it would allow addition of complex substituting oligo-/polysaccharides on a linear rhamnan backbone chain. Regarding *L. lactis* NZ9000, the three components would include (i) WpsA/WpsB to synthesize Und-P-GlcNAc and to initiate synthesis of an oligosaccharide PSP subunit further elongated by WpsC/D/E/F, (ii) the flippase WpsG to flip the Und-P-oligosaccharide to the outside of the membrane, and (iii) the polytopic membrane GT-C glycosyltransferase WpsJ to attach PSP to rhamnan. In the C-type strain *L. lactis* NZ9000, this modification mechanism is com-

bined with a polymerization step to synthesize PSP chains as modifying entities that are attached to rhamnan chains. We speculate that the polymerization step is performed by the GT-C-fold glycosyltransferase (WpsI) utilizing Und-P-PSP subunit as donor, with WpsH resembling a Wzz protein as the copolymerase and/or chain regulator. We hypothesize that the acceptor of this reaction would be the growing PSP polymeric chain linked to Und-P as represented in Fig. 5.

Interestingly, the two proteins WpsA and WpsB are highly conserved in *L. lactis* strains whatever their CWPS type (A, B, or C) (11, 12), and the corresponding genes are located in a similar position in the *wcps* cluster. Therefore, we propose that the model pathway described above may apply more generally to all *L. lactis* strains, with the two proteins WpsA/B initiating synthesis of the CWPS variable parts that are poly- or oligosaccharide chains by the transfer of GlcNAc on Und-P. Notably, in the three type C strains with known PSP structures, GlcNAc is present in a similar position compared with the phosphodiester bond (Fig. S1), suggesting a biosynthesis pathway very similar to that proposed for NZ9000. Regarding *L. lactis* IL1403 (type B CWPS), the side chain substituting rhamnan chains is composed of a trisaccharide with a GlcNAc at the reducing end. This trisaccharide could thus be synthesized in the cytoplasm on an Und-P lipid carrier, then transferred to the outside of the cell membrane by a flippase (detected in the corresponding IL1403 *wcps* variable part), and attached to rhamnan by a GT-C-fold glycosyltransferase encoded in a similar position as *wpsJ* in the IL1403 *wcps* locus (12). This model can also apply to the type A CWPS of *L. lactis* UC509.9 where the side-chain substituents contain a GlcNAc residue at their reducing end that is branched on the rhamnose-rich core chains (Fig. S1).

Rha-containing CWPSs are also synthesized by streptococci and enterococci where they constitute attractive vaccine candidates and/or are involved in pathogenesis (18, 19, 30). More recently, such a PS with a role in bacteria–host interactions was also found in *Ruminococcus gnavus*, an unrelated bacterial species of the gut microbiota (31), suggesting an even larger distribution. These Rha-containing CWPSs exhibit different levels of complexity, comprising a polyrhamnose backbone chain made of 1,3- and 1,2-linked L-Rha with either single monosaccharides as substituents or more complex side chains. We speculate that the biosynthesis scheme proposed here for *L. lactis* CWPS also applies to other complex Rha-containing CWPSs such as the Group B carbohydrate produced in *Streptococcus agalactiae* (18, 32). Interestingly and as highlighted previously (32), the Group B carbohydrate biosynthesis locus contains homologs of WpsA, WpsB, WpsH, and WpsI.

### Conclusions

The biosynthesis pathway proposed here for *L. lactis* CWPS accounts for the high structural diversity encountered in these glycopolymers among strains. Overall, the proposed scheme can be envisioned as an evolutionary refinement of the three-component mechanism described previously for extracytoplasmic modification of bacterial glycoconjugates by monosaccha-



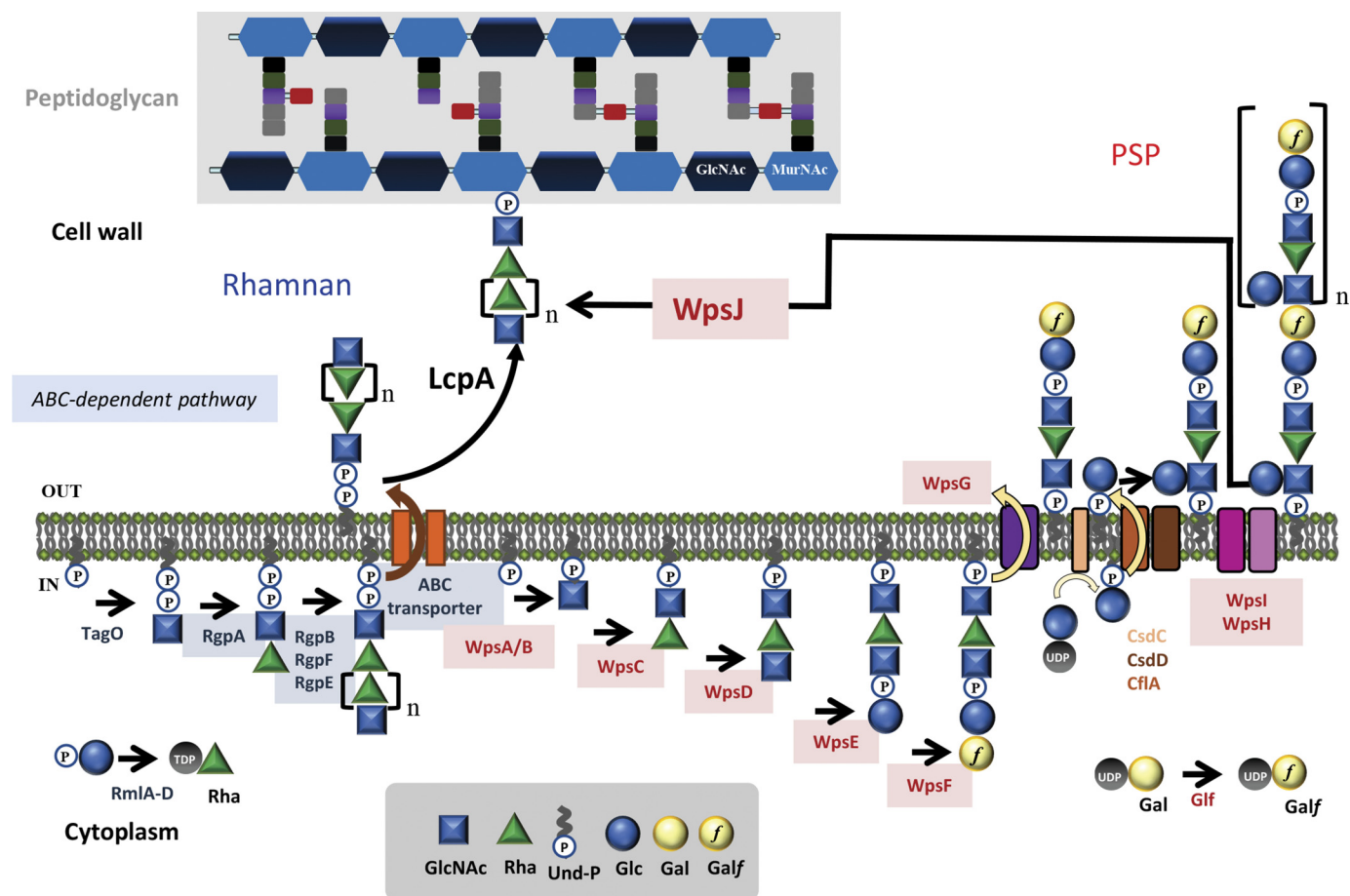


**Figure 5. Schematic of the proposed enzymatic pathway involved in the assembly of rhamnan and PSP of *L. lactis* NZ9000.** Left side, rhamnan. Rhamnan is synthesized intracellularly by an ABC-dependent pathway, initiated by the addition of GlcNAc-P on Und-P by TagO. The four enzymes RmlA, -B, -C, and -D are known to be involved in rhamnose precursor, dTDP-L-Rha, synthesis. Then the rhamnosyltransferase RgpA transfers the first rhamnosyl residue on the GlcNAc-P-Und lipid intermediate acceptor, and the chain is further elongated by two other rhamnosyltransferases, RgpB and RgpF, to reach an average length of 33 Rha residues (corresponding to 11 repeating units) and terminated by GlcNAc addition by RgpE. Together, RgpC and RgpD, constituting an ABC transporter, catalyze the transfer of the rhamnan chain to the outer side of the cytoplasmic membrane. Following export, the rhamnan is most probably anchored covalently to peptidoglycan acceptor sites, via a phosphodiester linkage to *N*-acetylmuramic acid (MurNAc) (or GlcNAc) residues of the glycan chains, with LcpA being the main ligase involved. Right side, PSP. Synthesis starts by transfer of GlcNAc on Und-P by WpsA/WpsB. The repeat unit is then synthesized on the GlcNAc-P-Und lipid precursor at the intracellular face of the cytoplasmic membrane by the successive addition of Rha, GlcNAc, Glc-P, and Galf catalyzed by the glycosyltransferases WpsC, WpsD, WpsE, and WpsF with UDP-Galf formed from UDP-Gal by Glf. According to our data,<sup>6</sup> the last sugar of the hexasaccharide repeat unit, the side-chain Glc, is added, presumably outside the cytoplasmic membrane, by a three-component glycosylation mechanism encoded outside the *cwps* cluster. The linear pentasaccharidic PSP repeat unit is flipped to the outside of the cytoplasmic membrane by the flippase WpsG. It is then polymerized by WpsI with WpsH as a putative copolymerase and/or chain-length regulator. Finally, WpsJ is involved in the transfer of the PSP onto rhamnan.

rides toward a system for the addition of complex substituting oligo-/polysaccharides onto the rhamnan. The site of linkage of PSP onto rhamnan and the nature of the bond remain to be determined. In addition, the spatiotemporal control of rhamnan anchoring to peptidoglycan by an Lcp ligase relative to PSP polymerization by WpsI/H and attachment on rhamnan by WpsJ remains to be investigated. These molecular events appear to be of special importance for the cell-wall assembly and cell division processes because *L. lactis* mutants impaired in PSP (Fig. 4) as well as in rhamnan synthesis (15) exhibit severe alterations of cell shape and septum positioning. Finally, the model for the CWPS assembly pathway presented here provides a framework to study further the functionalities of the individual glycosyltransferases and polysaccharide-assembly enzymes encoded by the various *cwps* gene clusters of *L. lactis* and other Gram-positive bacteria.

## Experimental procedures

### Strains and growth conditions

Bacterial strains used in this study are listed in Table S1. Strains were grown at 30 °C overnight in M17 broth and/or M17 agar (Oxoid Ltd., Hampshire, UK) supplemented with 5 g of glucose/liter or kg of M17 medium (GM17). Chloramphenicol (5 µg/ml), tetracycline (10 µg/ml), or erythromycin (5 µg/ml) (Sigma-Aldrich) was added to media where appropriate. For controlled transcription of genes placed under the nisin-inducible promoter, *P<sub>nisA</sub>*, the growth medium was supplemented with Nisaplin (DuPont) at a final concentration of 40 ng/ml.

### Promoter mapping

All recombinant plasmids (Table S1) were generated in *L. lactis* NZ9000, and the primers (Table S2), unless otherwise

indicated, were ordered from Eurofins MWG (Ebersberg, Germany). All intergenic regions present within the *cwps* gene cluster of strains *L. lactis* NZ9000, defined as the nucleotide sequence directly upstream of any annotated gene start codon and directly downstream of the upstream gene's annotated stop codon (>20 bp), were amplified using the oligonucleotides listed in Table S2 with Phusion® high-fidelity DNA polymerase (New England Biolabs) and cloned into the low-copy, promoter–probe vector pPTPL (33). The resulting constructs are listed in Table S1. Promoter activity was assessed visually by plating the *L. lactis* NZ9000 harboring the above-mentioned constructs onto GM17 agar plates containing 10 µg/ml X-gal (5-bromo-4-chloro-3-indolyl β-D-galactopyranoside; Sigma-Aldrich) as well as quantitatively by measuring their specific β-gal activity during early lag (1 h 15 min after subculture), mid-exponential (3 h 30 min after subculture), and late-exponential (6 h 30 min after subculture) phases of growth as described previously (33).

### Primer extension analysis

*L. lactis* NZ9000 harboring individual pPTPL constructs that were shown to exhibit promoter activity were subcultured in GM17 to an OD<sub>600 nm</sub> of ~0.1 and allowed to grow at 30 °C until the culture reached mid-exponential growth phase, after which total RNA was isolated using a method described previously (34) in combination with a High Pure RNA Isolation kit (Roche Diagnostics). Primer extension was performed as described previously (35). Sequence ladders of the presumed promoter regions immediately upstream of *llnz\_01075* (*rmlA*), *llnz\_01135* (*wpsA*), and *llnz\_01175* (*wpsH*) (of *L. lactis* NZ9000) were amplified from their respective pPTPL plasmid preparations. These sequence ladders were produced using primers (Table S2) that were also employed for the corresponding primer extension reaction using the Thermo Sequenase primer cycle sequencing kit (Amersham Biosciences). Separation of extension and sequencing products was achieved on a 10% LI-COR Matrix KB Plus acrylamide gel. Signal detection and image capture were performed in a LI-COR sequencing instrument (LI-COR Biosciences).

### RT-PCR

The transcriptional organization of the *cwps* gene cluster was confirmed using RT-PCR. Four independently grown cultures of *L. lactis* NZ9000 (20 ml) had their total RNA isolated (at an OD<sub>600 nm</sub> of ~0.5) using a method described previously (34) in combination with a High Pure RNA Isolation kit. The RNA was then reverse transcribed into cDNA using SuperScript™ III reverse transcriptase (Invitrogen) along with a 9-bp-long random-nucleotide primer according to the manufacturer's instructions. The final cDNA preparation was used as a template to confirm the transcriptional separation (or connection by means of transcriptional read-through) of particular *cwps* genes by means of a PCR targeting the regions directly upstream and downstream of the identified *cwps* promoters (Fig. S3). Regions within each deduced transcriptional unit were subjected to cDNA-based PCR amplification to serve as a positive control, whereas cDNA corresponding to regions

upstream and downstream of the complete gene cluster were targeted by PCR as a negative control (Fig. S3).

### CRISPR recombineering

CRISPR–Cas9-assisted recombineering was adapted from a method published previously (36) and applied to generate mutations in 15 of the 22 identified genes of the *cwps* gene cluster of *L. lactis* NZ9000, whereas two mutants (NZ9000-*wpsA* and NZ9000-*wpsH*) were obtained using the classical recombineering method (37). The system was not applied to genes that are proposed to be involved in the dTDP-L-rhamnose biosynthetic pathway (*rmlA*, *rmlB*, *rmlX*, *rmlC*, and *rmlD*) as they are presumed to be essential for bacterial growth. Briefly, plasmid pCNR, which contains the replication functions of the pPTPi plasmid (38) along with the chloramphenicol resistance gene (*cm<sup>r</sup>*), *P<sup>nisA</sup>* promoter, and the single-stranded DNA-binding protein-encoding gene *recT* from plasmid pJP005 (37), was constructed. Subsequently, the single-step approach to CRISPR–Cas9-assisted recombineering was employed as outlined previously (38) (Fig. S4). Electrocompetent cells of *L. lactis* NZ9000 carrying both pVPL3004 (expressing Cas9 and transactivating CRISPR RNA) and pCNR (RecT-expressing plasmid) were prepared as described previously (37). These cells were then cotransformed with both 100 µg of a particular recombineering oligonucleotide (Table S3) and 100 ng of the corresponding pCRISPR construct (Table S1). After recovery, cells were plated on GM17 agar plates supplemented with tetracycline (10 µg/ml) and erythromycin (5 µg/ml), selecting for plasmids pVPL3004 and pCRISPR. Colonies were screened using colony PCR, and those containing the appropriate disruptive sequence insertion were further purified (Table S2). The recombineering oligonucleotides were ordered from Integrated DNA Technologies (Leuven, Belgium). Nine mutants were successfully obtained (Table S1).

### Bioinformatics analysis

Integrated Microbial Genomes and Microbiomes System v.5.0 (<https://img.jgi.doe.gov/m/>) was used to assign functions to proteins encoded in the *cwps* cluster. Sequence homology search was performed with BlastP, and structural prediction was made with the use of HHpred (<https://toolkit.tuebingen.mpg.de/tools/hhpred>).<sup>7</sup> Membrane topology was assessed by TMHMM v.2.0.

### CWPS structural analysis

Bacteria were harvested from an exponentially growing culture at an OD<sub>600 nm</sub> of 0.6, and cell walls were prepared as described previously (39). Briefly, heat-killed bacteria were boiled in 5% SDS, and the pellet, recovered by centrifugation, was treated successively by Pronase and trypsin to remove proteins and RNase and DNase to remove nucleic acids. The resulting material corresponding to purified cell walls (containing peptidoglycan and CWPS) was treated with 48% HF for 48 h at 4 °C to extract CWPS. The samples were centrifuged at 20,000 × *g*, and the supernatant containing CWPS was dried

<sup>7</sup> Please note that the JBC is not responsible for the long-term archiving and maintenance of this site or any other third party hosted site.

under a stream of nitrogen. The residue was solubilized in Milli-Q H<sub>2</sub>O and lyophilized. Rhamnan and PSP oligosaccharides present in the sample were separated by SEC–HPLC with two columns in tandem (Shodex Sugar KS-804 and KS-803 columns, Showa Denko, Japan) as described previously (15). Elution was performed with Milli-Q H<sub>2</sub>O, and detection of eluted compounds was performed with a refractometer (2414 Refractive Index Detector, Waters) and/or a UV detector at 206 nm. Fractions corresponding to peaks containing rhamnan and PSP oligosaccharides were collected and dried under vacuum. They were further analyzed by MALDI-TOF MS using 2,5-dihydroxybenzoic acid matrix with an UltrafleXtreme instrument (Bruker Daltonics).

## TEM

Samples were fixed with 2% glutaraldehyde in 0.1 M sodium cacodylate buffer, pH 7.2, for 1 h at room temperature. Samples were then contrasted with 0.5% Oolong tea extract in cacodylate buffer, postfixed with 1% osmium tetroxide containing 1.5% potassium cyanoferrate, gradually dehydrated in ethanol (30–100%), substituted gradually in an ethanol–Epon mixture, and embedded in Epon (DELTA Microscopies, France). Thin sections (70 nm) were collected onto 200-mesh copper grids and counterstained with lead citrate. Grids were examined with a Hitachi HT7700 electron microscope operated at 80 kV, and images were acquired with a charge-coupled device camera (Advanced Microscopy Techniques) (facilities located on the MIMA2 platform, INRA, AgroParisTech, Jouy-en-Josas, France).

## Bacteriophage assays and isolation of bacteriophage escape mutants

Phages used in this study are listed in Table S1. Propagation of phages on their respective host strains was performed as described previously (40). Similarly, both spot/plaque assays (41) and adsorption assays (42) were performed as described previously. Phage escape mutants (Table S1) derived from the 936 group phage sk1 (NC\_001835.1) and capable of infecting the PSP-deficient derivative of *L. lactis* MG1363 (VES5751) (13) were also isolated. The general procedure for isolation of phage mutants able to infect the *L. lactis* VES5751 strain was as follows. Exponentially growing *L. lactis* MG1363 cells (2 ml) were infected with sk1 with a multiplicity of infection of 5 and incubated for 15 min at 30 °C. Free phages were then removed by centrifugation at 4,000 rpm for 4 min at 4 °C. The cellular pellet was resuspended in 100 µl of fresh GM17 medium supplemented with 10 mM CaCl<sub>2</sub> and mixed with an equal volume of *L. lactis* VES5751 cells. Phage mutants able to infect *L. lactis* VES5751 and forming visible plaques on this PSP-deficient strain were isolated using the double-agar overlay method and retested for their ability to efficiently infect *L. lactis* VES5751.

Genomic DNA of the eight isolated, sk1-derived escape mutants (Table S1) was extracted as described previously (43) and fully sequenced to identify the mutations allowing these escape mutants to propagate on *L. lactis* VES5751. Genome sequencing was performed using Illumina MiSeq sequencing technology (GenProbio, Parma, Italy). The MEGAnnotator pipeline was used for *de novo* sequence assemblies as well as automated gene calling (44), and putative open reading frames

(ORFs) were assigned via Prodigal v2.6 and GeneMark.hmm (45).

**Author contributions**—I. T., S. K., J. M., D. v. S., and M.-P. C.-C. conceptualization; I. T., P. C., S. P., E. B., C. Péchoux, and C. Penno investigation; I. T., P. C., S. P., S. K., E. B., C. Péchoux, F. F., and M.-P. C.-C. methodology; I. T. and M.-P. C.-C. writing-original draft; F. F. resources; F. F., D. v. S., and M.-P. C.-C. validation; J. M., D. v. S., and M.-P. C.-C. supervision; J. M., D. v. S., and M.-P. C.-C. funding acquisition; J. M., D. v. S., and M.-P. C.-C. writing-review and editing; M.-P. C.-C. data curation.

## References

1. Chapot-Chartier, M. P., and Kulakauskas, S. (2014) Cell wall structure and function in lactic acid bacteria. *Microb. Cell Fact.* **13**, Suppl. 1, S9 [CrossRef Medline](#)
2. Tytgat, H. L., and Lebeer, S. (2014) The sweet tooth of bacteria: common themes in bacterial glycoconjugates. *Microbiol. Mol. Biol. Rev.* **78**, 372–417 [CrossRef Medline](#)
3. Mostowy, R. J., and Holt, K. E. (2018) Diversity-generating machines: genetics of bacterial sugar-coating. *Trends Microbiol.* **26**, 1008–1021 [CrossRef Medline](#)
4. Woodward, L., and Naismith, J. H. (2016) Bacterial polysaccharide synthesis and export. *Curr. Opin. Struct. Biol.* **40**, 81–88 [CrossRef Medline](#)
5. Yother, J. (2011) Capsules of *Streptococcus pneumoniae* and other bacteria: paradigms for polysaccharide biosynthesis and regulation. *Annu. Rev. Microb.* **65**, 563–581 [CrossRef Medline](#)
6. Cuthbertson, L., Kos, V., and Whitfield, C. (2010) ABC transporters involved in export of cell surface glycoconjugates. *Microbiol. Mol. Biol. Rev.* **74**, 341–362 [CrossRef Medline](#)
7. Kawai, Y., Marles-Wright, J., Cleverley, R. M., Emmins, R., Ishikawa, S., Kuwano, M., Heinz, N., Bui, N. K., Hoyland, C. N., Ogasawara, N., Lewis, R. J., Vollmer, W., Daniel, R. A., and Errington, J. (2011) A widespread family of bacterial cell wall assembly proteins. *EMBO J.* **30**, 4931–4941 [CrossRef Medline](#)
8. Mann, E., and Whitfield, C. (2016) A widespread three-component mechanism for the periplasmic modification of bacterial glycoconjugates. *Can. J. Chem.* **94**, 883–893 [CrossRef](#)
9. Cavanagh, D., Fitzgerald, G. F., and McAuliffe, O. (2015) From field to fermentation: the origins of *Lactococcus lactis* and its domestication to the dairy environment. *Food Microbiol.* **47**, 45–61 [CrossRef Medline](#)
10. Mahony, J., Cambillau, C., and van Sinderen, D. (2017) Host recognition by lactic acid bacterial phages. *FEMS Microbiol. Rev.* **41**, S16–S26 [CrossRef Medline](#)
11. Ainsworth, S., Sadovskaya, I., Vinogradov, E., Courtin, P., Guerardel, Y., Mahony, J., Grard, T., Cambillau, C., Chapot-Chartier, M. P., and van Sinderen, D. (2014) Differences in lactococcal cell wall polysaccharide structure are major determining factors in bacteriophage sensitivity. *mBio* **5**, e00880-14 [CrossRef Medline](#)
12. Mahony, J., Kot, W., Murphy, J., Ainsworth, S., Neve, H., Hansen, L. H., Heller, K. J., Sørensen, S. J., Hammer, K., Cambillau, C., Vogensen, F. K., and van Sinderen, D. (2013) Investigation of the relationship between lactococcal host cell wall polysaccharide genotype and 936 phage receptor binding protein phylogeny. *Appl. Environ. Microbiol.* **79**, 4385–4392 [CrossRef Medline](#)
13. Chapot-Chartier, M. P., Vinogradov, E., Sadovskaya, I., Andre, G., Mistou, M. Y., Trieu-Cuot, P., Furlan, S., Bidnenko, E., Courtin, P., Péchoux, C., Hols, P., Dufrène, Y. F., and Kulakauskas, S. (2010) The cell surface of *Lactococcus lactis* is covered by a protective polysaccharide pellicle. *J. Biol. Chem.* **285**, 10464–10471 [CrossRef Medline](#)
14. Farenc, C., Spinelli, S., Vinogradov, E., Tremblay, D., Blangy, S., Sadovskaya, I., Moineau, S., and Cambillau, C. (2014) Molecular insights on the recognition of a *Lactococcus lactis* cell wall pellicle by the phage 1358 receptor binding protein. *J. Virol.* **88**, 7005–7015 [CrossRef Medline](#)
15. Sadovskaya, I., Vinogradov, E., Courtin, P., Armalyte, J., Meyrand, M., Giaouris, E., Palussière, S., Furlan, S., Péchoux, C., Ainsworth, S., Mahony,



- J., van Sinderen, D., Kulakauskas, S., Guérardel, Y., and Chapot-Chartier, M. P. (2017) Another brick in the wall: a rhamnan polysaccharide trapped inside peptidoglycan of *Lactococcus lactis*. *mBio* **8**, e01303-17 [CrossRef Medline](#)
16. Vinogradov, E., Sadovskaya, I., Courtin, P., Kulakauskas, S., Grard, T., Mahony, J., van Sinderen, D., and Chapot-Chartier, M. P. (2018) Determination of the cell wall polysaccharide and teichoic acid structures from *Lactococcus lactis* IL1403. *Carbohydr. Res.* **462**, 39–44 [CrossRef Medline](#)
  17. Vinogradov, E., Sadovskaya, I., Grard, T., Murphy, J., Mahony, J., Chapot-Chartier, M. P., and van Sinderen, D. (2018) Structural studies of the cell wall polysaccharide from *Lactococcus lactis* UC509.9. *Carbohydr. Res.* **461**, 25–31 [CrossRef Medline](#)
  18. Mistou, M. Y., Sutcliffe, I. C., and van Sorge, N. M. (2016) Bacterial glyco-biology: rhamnose-containing cell wall polysaccharides in Gram-positive bacteria. *FEMS Microbiol. Rev.* **40**, 464–479 [CrossRef Medline](#)
  19. van Sorge, N. M., Cole, J. N., Kuipers, K., Henningham, A., Aziz, R. K., Kasirer-Friede, A., Lin, L., Berends, E. T. M., Davies, M. R., Dougan, G., Zhang, F., Dahesh, S., Shaw, L., Gin, J., Cunningham, M., et al. (2014) The classical Lancefield antigen of group A *Streptococcus* is a virulence determinant with implications for vaccine design. *Cell Host Microbe* **15**, 729–740 [CrossRef Medline](#)
  20. Caliot, É., Dramsi, S., Chapot-Chartier, M. P., Courtin, P., Kulakauskas, S., Péchoux, C., Trieu-Cuot, P., and Mistou, M. Y. (2012) Role of the Group B antigen of *Streptococcus agalactiae*: a peptidoglycan-anchored polysaccharide involved in cell wall biogenesis. *PLoS Pathog.* **8**, e1002756 [CrossRef Medline](#)
  21. van der Meulen, S. B., de Jong, A., and Kok, J. (2016) Transcriptome landscape of *Lactococcus lactis* reveals many novel RNAs including a small regulatory RNA involved in carbon uptake and metabolism. *RNA Biol.* **13**, 353–366 [CrossRef Medline](#)
  22. Lukose, V., Walvoort, M. T. C., and Imperiali, B. (2017) Bacterial phosphoglycosyl transferases: initiators of glycan biosynthesis at the membrane interface. *Glycobiology* **27**, 820–833 [CrossRef Medline](#)
  23. Larkin, A., Chang, M. M., Whitworth, G. E., and Imperiali, B. (2013) Biochemical evidence for an alternate pathway in N-linked glycoprotein biosynthesis. *Nat. Chem. Biol.* **9**, 367–373 [CrossRef Medline](#)
  24. Rush, J. S., Edgar, R. J., Deng, P., Chen, J., Zhu, H., van Sorge, N. M., Morris, A. J., Korotkov, K. V., and Korotkova, N. (2017) The molecular mechanism of N-acetylglucosamine side-chain attachment to the Lancefield group A carbohydrate in *Streptococcus pyogenes*. *J. Biol. Chem.* **292**, 19441–19457 [CrossRef Medline](#)
  25. Lairson, L. L., Henrissat, B., Davies, G. J., and Withers, S. G. (2008) Glycosyltransferases: structures, functions, and mechanisms. *Annu. Rev. Biochem.* **77**, 521–555 [CrossRef Medline](#)
  26. Islam, S. T., and Lam, J. S. (2014) Synthesis of bacterial polysaccharides via the Wzx/Wzy-dependent pathway. *Can. J. Microbiol.* **60**, 697–716 [CrossRef Medline](#)
  27. Giraud, M. F., and Naismith, J. H. (2000) The rhamnose pathway. *Curr. Opin. Struct. Biol.* **10**, 687–696 [CrossRef Medline](#)
  28. McCabe, O., Spinelli, S., Farenc, C., Labbé, M., Tremblay, D., Blangy, S., Oscarson, S., Moineau, S., and Cambillau, C. (2015) The targeted recognition of *Lactococcus lactis* phages to their polysaccharide receptors. *Mol. Microbiol.* **96**, 875–886 [CrossRef Medline](#)
  29. Bebeacua, C., Tremblay, D., Farenc, C., Chapot-Chartier, M. P., Sadovskaya, I., van Heel, M., Veeler, D., Moineau, S., and Cambillau, C. (2013) Structure, adsorption to host, and infection mechanism of virulent lactococcal phage p2. *J. Virol.* **87**, 12302–12312 [CrossRef Medline](#)
  30. Rigottier-Gois, L., Madec, C., Navickas, A., Matos, R. C., Akary-Lepage, E., Mistou, M. Y., and Serror, P. (2015) The surface rhamnopolysaccharide epa of *Enterococcus faecalis* is a key determinant of intestinal colonization. *J. Infect. Dis.* **211**, 62–71 [CrossRef Medline](#)
  31. Henke, M. T., Kenny, D. J., Cassilly, C. D., Vlamakis, H., Xavier, R. J., and Clardy, J. (2019) *Ruminococcus gnavus*, a member of the human gut microbiome associated with Crohn's disease, produces an inflammatory polysaccharide. *Proc. Natl. Acad. Sci. U.S.A.* **116**, 12672–12677 [CrossRef Medline](#)
  32. Sutcliffe, I. C., Black, G. W., and Harrington, D. J. (2008) Bioinformatic insights into the biosynthesis of the Group B carbohydrate in *Streptococcus agalactiae*. *Microbiology* **154**, 1354–1363 [CrossRef Medline](#)
  33. Israelsen, H., Madsen, S. M., Vrang, A., Hansen, E. B., and Johansen, E. (1995) Cloning and partial characterization of regulated promoters from *Lactococcus lactis* Tn917-lacZ integrants with the new promoter probe vector, pAK80. *Appl. Environ. Microbiol.* **61**, 2540–2547 [CrossRef Medline](#)
  34. Kuipers, O. P., Beerthuyzen, M. M., Siezen, R. J., and De Vos, W. M. (1993) Characterization of the nisin gene cluster *nisABTCIPR* of *Lactococcus lactis*. Requirement of expression of the *nisA* and *nisI* genes for development of immunity. *Eur. J. Biochem.* **216**, 281–291 [CrossRef Medline](#)
  35. Ventura, M., Zink, R., Fitzgerald, G. F., and van Sinderen, D. (2005) Gene structure and transcriptional organization of the *dnaK* operon of *Bifidobacterium breve* UCC 2003 and application of the operon in bifidobacterial tracing. *Appl. Environ. Microbiol.* **71**, 487–500 [CrossRef Medline](#)
  36. Oh, J. H., and van Pijkeren, J. P. (2014) CRISPR-Cas9-assisted recombineering in *Lactobacillus reuteri*. *Nucleic Acids Res.* **42**, e131 [CrossRef Medline](#)
  37. van Pijkeren, J. P., and Britton, R. A. (2012) High efficiency recombineering in lactic acid bacteria. *Nucleic Acids Res.* **40**, e76 [CrossRef Medline](#)
  38. O'Driscoll, J., Glynn, F., Cahalane, O., O'Connell-Motherway, M., Fitzgerald, G. F., and Van Sinderen, D. (2004) Lactococcal plasmid pNP40 encodes a novel, temperature-sensitive restriction-modification system. *Appl. Environ. Microbiol.* **70**, 5546–5556 [CrossRef Medline](#)
  39. Meyrand, M., Boughammoura, A., Courtin, P., Mézange, C., Guillot, A., and Chapot-Chartier, M. P. (2007) Peptidoglycan N-acetylglucosamine deacetylation decreases autolysis in *Lactococcus lactis*. *Microbiology* **153**, 3275–3285 [CrossRef Medline](#)
  40. Mahony, J., McGrath, S., Fitzgerald, G. F., and van Sinderen, D. (2008) Identification and characterization of lactococcal-phage-carried superinfection exclusion genes. *Appl. Environ. Microbiol.* **74**, 6206–6215 [CrossRef Medline](#)
  41. Lillehaug, D. (1997) An improved plaque assay for poor plaque-producing temperate lactococcal bacteriophages. *J. Appl. Microbiol.* **83**, 85–90 [CrossRef Medline](#)
  42. Ostergaard Breum, S., Neve, H., Heller, K. J., and Vogensen, F. K. (2007) Temperate phages TP901-1 and  $\phi$ LC3, belonging to the P335 species, apparently use different pathways for DNA injection in *Lactococcus lactis* subsp. *cremoris* 3107. *FEMS Microbiol. Lett.* **276**, 156–164 [CrossRef Medline](#)
  43. Lavelle, K., Martinez, I., Neve, H., Lugli, G. A., Franz, C. M. A. P., Ventura, M., Bello, F. D., Sinderen, D. V., and Mahony, J. (2018) Biodiversity of *Streptococcus thermophilus* phages in global dairy fermentations. *Viruses* **10**, E577 [CrossRef Medline](#)
  44. Lugli, G. A., Milani, C., Mancabelli, L., van Sinderen, D., and Ventura, M. (2016) MEGAnnotator: a user-friendly pipeline for microbial genomes assembly and annotation. *FEMS Microbiol. Lett.* **363**, fnw049 [CrossRef Medline](#)
  45. Besemer, J., and Borodovsky, M. (1999) Heuristic approach to deriving models for gene finding. *Nucleic Acids Res.* **27**, 3911–3920 [CrossRef Medline](#)
  46. Shibata, Y., Yamashita, Y., Ozaki, K., Nakano, Y., and Koga, T. (2002) Expression and characterization of streptococcal *rgp* genes required for rhamnan synthesis in *Escherichia coli*. *Infect. Immun.* **70**, 2891–2898 [CrossRef Medline](#)
  47. Sperisen, P., Schmid, C. D., Bucher, P., and Zilian, O. (2005) Stealth proteins: *in silico* identification of a novel protein family rendering bacterial pathogens invisible to host immune defense. *PLoS Comput. Biol.* **1**, e63 [CrossRef Medline](#)